JPhys Energy

TOPICAL REVIEW • OPEN ACCESS

# Nanoscale differentiation of surfaces and cores for olivine phosphate particles—a key characteristic of practical battery materials

Journal of Physics: Energy

TOPICAL REVIEW

# Nanoscale differentiation of surfaces and cores for olivine phosphate particles—a key characteristic of practical battery materials

Y Zhang[1], J A Alarco, M Khosravi and I D R Mackinnon

Institute for Future Environments and Science and Engineering Faculty, Queensland University of Technology (QUT), Brisbane, QLD 4001, Australia

[1] Current address: CRRC Qingdao Sifang Co., Ltd, Qingdao 266 111, China

**E-mail:** jose.alarco@qut.edu.au

**Keywords:** band gap, lithium-ion batteries, olivine phosphates, cathode materials, DFT, electronic band structure, surface

OPEN ACCESS

RECEIVED
7 October 2020

REVISED
21 December 2020

ACCEPTED FOR PUBLICATION
3 February 2021

PUBLISHED
6 April 2021



## Abstract

We provide a review of our recent studies on the surface chemistries and electronic structures of olivine phosphate cathode materials $LiMPO_4$ (M = Mn, Fe, Co, Ni). Li-depletion and mixed oxidation for the transition metal ions have been detected on particle surfaces, across the family of metal phosphate cathode materials. The effects of surface Li-depletion on optical properties and electronic band structures are discussed. $LiFePO_4$ doped with metals or ions that are reported in the literature as beneficial for rate capability enhancement show more pronounced surface Li-depletion and mixed oxidation compared to undoped material. This outcome, among others, indicates that the dopant resides predominantly on, and influences, the surface of cathode materials.

## 1. Introduction

Efficient and economic energy conversion and storage have become critical to addressing current global environmental concerns and resource shortages. Li-ion batteries (LIBs) are reversible energy storage devices, that have drawn much attention from industry and academia in recent years. Since the original work of Goodenough *et al* on $LiFePO_4$ (LFP) [1], $LiMPO_4$ (M = Mn, Fe, Co, Ni) materials with olivine structure have been considered as among the most promising candidates for cathode materials due to their superiority in electrochemical performance, thermal stability and environmental compatibility. However, high-rate applications of phosphate materials have been greatly inhibited by their poor electronic conductivity ($10^{-13}$–$10^{-16}$ $cm^2$ $s^{-1}$) and slow diffusion of $Li^+$ ($\sim 10^{-9}$ S $cm^{-1}$) [2–4]. Accordingly, multiple efforts have been made to improve the electronic and ionic conductivities of $LiMPO_4$, such as by applying conductive surface coatings [5–8], particle size reduction [9, 10], composite electrode preparation [11–13] and doping [14–16].

As the interface to the electrolyte and the gateway for Li-ion transfer, the surfaces of the electrode materials play an important role in the performance of LIBs [17], and their detailed characterization is receiving more focused research attention. Although many efforts have been made to improve the electronic and ionic conductivities of $LiMPO_4$, the surfaces of the olivine phosphates still require detailed characterization. In this paper, an overview of our recent investigations on surface characteristics and their effects on the electronic band structures for $LiMPO_4$ materials is presented.

This article is based on the PhD thesis work of Ms Yin Zhang, recently awarded the degree [18]. Detailed descriptions of many sections in this review have already been published [19–24] or are in preparation for separate submissions. However, the authors in consultation with the journal editors, considered appropriate to write an overview that combines and connects, in a logical, coherent fashion, various aspects of this work. We also add indicative modelling studies that suggest an effective pathway to intentional design of battery materials.

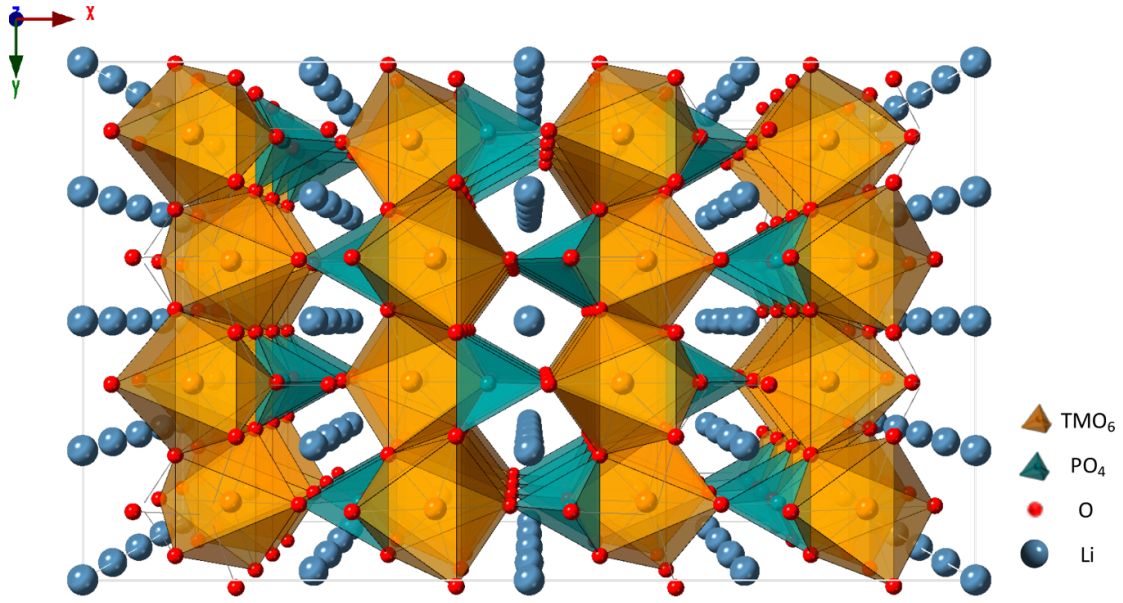


**Figure 1.** Crystal structure of olivine $LiMPO_4$ (M = Mn, Fe, Co and Ni).

## 2. Brief background to $LiMPO_4$

Olivine phosphates, typified by LFP, have orthorhombic unit cell with Pnma space group (number 62). The crystal structure symmetry can be represented as shown in figure 1 [25], containing four formula units. The transition metal ions with formal valency 2+ are the electrochemically active centres, which are oxidised to valency 3+ with the extraction of $Li^+$ and removal of associated electrons [26]. In the ordered olivine structure, the oxygen (O) ions form strong covalent bonds with phosphorus (P), in a stable three-dimensional framework, which provides safety under extreme conditions [27]. However, the strong covalent O bonds also lead to low ionic diffusivity and poor electronic conductivity [28]. Computational [29, 30] and experimental studies [31] on LFP have suggested that the more favourable diffusion path for Li is along the *b* axis. This favoured diffusion path is a slightly curved, one dimensional chain, that can be easily blocked by impurity atoms [30].

Among the family of $LiMPO_4$, LFP and LFP-based LIBs have been applied in industry for over 15 years [32]. LFP has a theoretical capacity of 170 mAh $g^{-1}$ with a flat operating voltage at 3.45 V vs $Li^+$/Li. The stability of the de-lithiated compound, $FePO_4$, allows for the full withdrawal of Li ions [1]. The other olivine phosphates exhibit higher operating voltage (4.1 V for $LiMnPO_4$ (LMP) [33], 4.8 V for $LiCoPO_4$ (LCP) [34] and 5.1 V for $LiNiPO_4$ (LNP) [35]) making them potential cathode materials for advanced LIBs, once issues with electrolyte stability at higher voltage plateaus are addressed. However, the extremely low intrinsic electronic conductivities of these materials greatly inhibit their electrochemical performance. Therefore, it is critical to understand the transport mechanism in order to improve the rate capability of olivine phosphate materials.

## 3. Electronic band structure and transport mechanism

Polaron hopping, which is a thermally activated process, not directly associated with the electronic band structure, has been reported as the major transport mechanism for LFP [26]. However, improvements to transport properties, for example via doping, may modify the electronic band structure and enhance band contributions to the transport behaviour. It is therefore of practical interest to gather knowledge on the electronic band structure of LFP and related phases, even if only as a benchmark for subsequent modification of the structure.

An important means to evaluate electronic conductivity of semiconductors includes the electronic band gap; for the same reason, band gaps should also be investigated for battery materials. The band gap value is also a convenient parameter for comparisons between experimentally determined and calculated values; thus, validating source calculations. The experimental band gaps reported in the literature for a selection of $LMPO_4$ materials are summarized in table 1. There is large disagreement on the experimental band gap values for LFP and for its de-lithiated phase. Table 1 also shows that these properties for other $LiMPO_4$

**Table 1.** Experimental band gaps for olivine phosphates reported in literature.

| | Method | Band gap | Reference |
|---|---|---|---|
| $LiFePO_4$ | UV–Vis | 3.8–4.0 eV | [36] |
| | UV–Vis | 3.84 eV | [37] |
| | UV–Vis | 4.8 eV, but no significant absorption before 5.8 eV | [38] |
| | XAS and RIXS | <0.95 eV | [39] |
| | XAS and XES | 4.0 or 0.5 eV | [40] |
| $FePO_4$ | UV–Vis | 1.88 eV | [37] |
| | XAS and XES | 1.7 eV | [40] |
| | UV–Vis | ~3.0 eV | [38] |
| $LiMnPO_4$ | XAS and XES | 4.0 eV | [41] |

Note: UV–Vis = ultraviolet-visible spectroscopy, XAS = x-ray absorption spectroscopy, RIXS = resonant inelastic x-ray scattering, XES = x-ray emission spectroscopy. Adapted from Zhang *et al*, RSC Advances [19], published by the Royal Society of Chemistry.

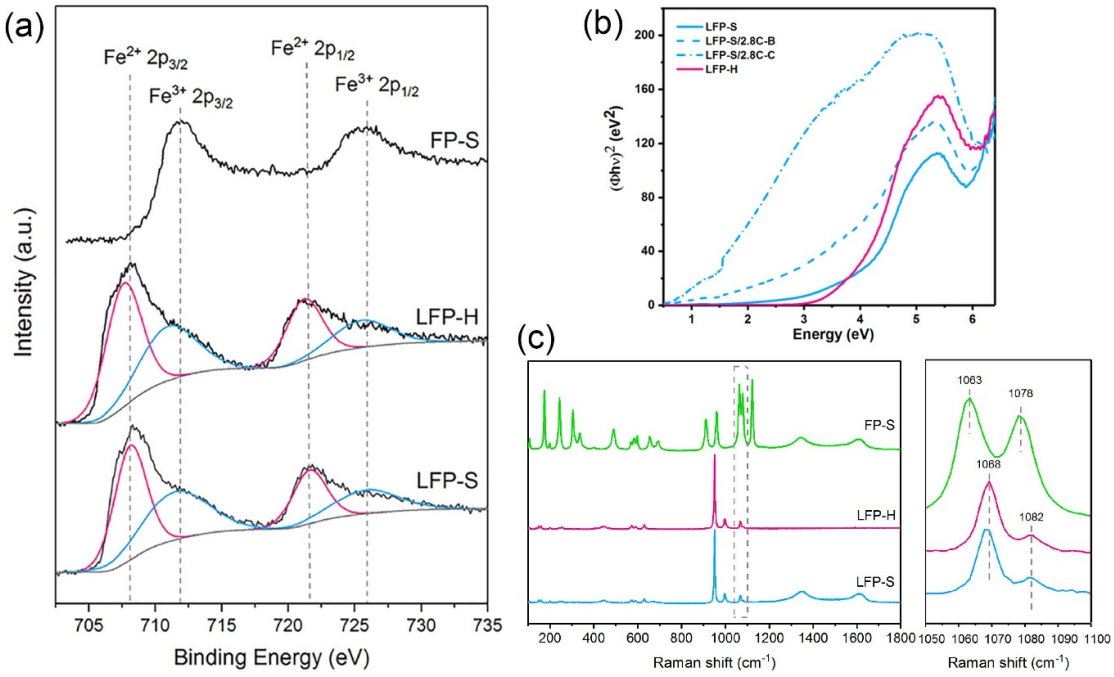


**Figure 2.** (a) XPS spectra, (b) Tauc plot and (c) Raman spectra for LFP and its de-lithiated samples. H refers to hydrothermally synthesized and S refers to solid-state synthesized samples. In figure 2(b) samples designated 2.8 C-B and 2.8 C-C are mechanically blended or coated with 2.8 wt% carbon. Adapted from [19]. CC BY 4.0.

materials have not been determined and require further investigation. Therefore, we have made systematic efforts to gain further knowledge on the electronic band gap of various transition metal olivine phosphates [19, 21, 23].

Investigations on LFP and its de-lithiated phase have been revisited [19] and Tauc plots from this work are shown in figure 2. Unlike the results reported in previous literature [36, 37], which appear to be measured on LFP samples synthesized using a solution or hydrothermal method [19], for nanoparticles with lower carbon content the absorbance rises gradually in the range of 1.7 eV–5 eV, with no sharp absorption edges in the measured energy range. The large Urbach tails shift greatly with the presence of small nanoscale amounts of additional carbon, which makes the large Urbach tails look like a surface related absorption from comparable nanoscale surface dimensions. These observations are in contrast to previous studies using alternative preparation methods for LFP. Therefore, a detailed investigation of the surface chemistry was undertaken using x-ray photoelectron spectroscopy (XPS) and Raman spectroscopy. As illustrated in figure 2, a mode related to the antisymmetric stretching of $PO_4^{3-}$ anion due to Li deficiency and a substantial fraction of $Fe^{3+}$ (where nominally there should only be $Fe^{2+}$) has been detected using both forms of spectroscopy. These data confirm the existence of Li depletion and $Fe^{3+}$ on the surface of LFP.

These types of investigations have been extended to the family of $LiMPO_4$ [21, 23]. The presence of both surface Li-depletion and $TM^{3+}$ have been further confirmed with synchrotron-based soft x-ray absorption

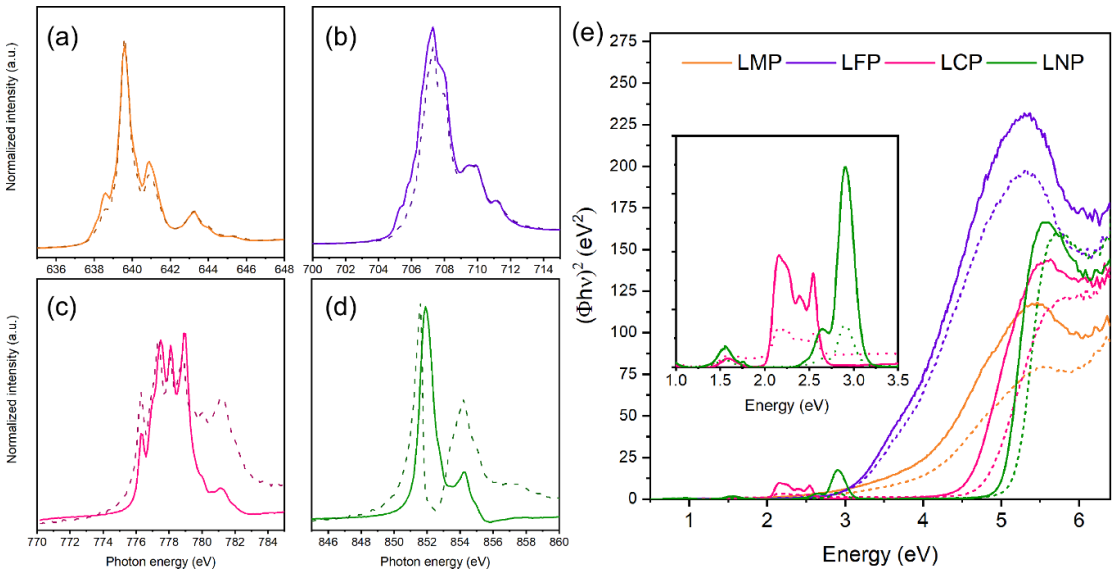


**Figure 3.** TM-$L_3$ edges for $LiMPO_4$ samples obtained with sXAS. (a) Mn-$L_3$, (b) Fe-$L_3$, (c) Co-$L_3$ and (d) Ni-$L_3$. The solid lines depict spectra acquired with TEY mode, while the dash lines depict spectra acquired with PEY mode. (e) The Tauc plot of the pristine (solid lines) and ground (dotted lines) $LiMPO_4$ samples. Reprinted (adapted) with permission from [21]. Copyright (2020) American Chemical Society.

spectroscopy (sXAS), as shown in figures 3(a)–(d). The total electron yield (TEY), partial electron yield (PEY) and total fluorescence yield (TFY) modes have been used to collect the near-edge x-ray absorption fine structures (NEXAFS) spectra. The TFY mode collects signal from the fluorescent x-rays with an escape depth of ∼3000 Å, whereas the EY modes collect signal from the Auger electrons with an escape depth of 50 Å. Consequently, the TFY mode gives information about the bulk, while the EY mode yields information near the surface [42]. The PEY mode filters Auger electrons with higher energy, which generally originate from the very surface of the particles, which makes PEY mode even more surface-sensitive compared with the TEY mode [43]. Therefore, both surface and bulk information can be obtained by simultaneously acquiring the PEY, TEY and TFY signals. Since the technique is depth sensitive [42, 43], the line shape difference within different modes indicates the difference in oxidation state of a TM ion with respect to the detection depth.

The effect of surface chemistry on the electronic structure has also been investigated by comparing the diffusive reflectance spectra of the pristine and ground $LiMPO_4$ samples. As shown in figure 3(e), after grinding, the intermediate absorptions in the visible energy range are weakened significantly and the main absorption edges are shifted to higher energy ranges for all the $LiMPO_4$ samples. After all the evidence is taken into consideration and following a similar perspective to that for LFP, band gaps of 4.6 eV for LCP and 5.1 eV for LNP can be determined.

## 4. Experimental validation of EBS calculations

With the experimental band gaps obtained in preliminary studies, the functionals within density functional theory (DFT) have been validated. The full comparison of GGA, GGA + U, HSE06 and sX-LDA have been reported in separate publications [19, 23]. In this brief review, a comparison of HSE06 and sX-LDA, two recommended hybrid functionals for more accurate band gap calculations [44, 45], is highlighted. The estimated electronic band structures and density of states with antiferromagnetic configurations are shown in figure 4.

Band gap estimations with the sX-LDA functional show a better agreement with the experimental optical gaps for all the olivine phosphates, except for LNP, which appears to have reported crystal information files (.cif) with small differences between reported values and slightly large weighted profile refinement R-factor [46–48]. Evaluating the structure with DFT, it also appears that the atoms represented by the .cif file have large residual non-equilibrium forces. A calculated band gap value for $FePO_4$ using sX-LDA (3.3 eV) matches the sharp optical absorption edge better than previously reported calculations [19]. Calculated values for LFP using sX-LDA (6.2 eV) also matches electron energy loss spectroscopy results very well. Remarkably, ultraviolet photoemission spectroscopy results, which allow for ionization potential and work function estimations, indicate that LFP has a negative electron affinity; that is, its vacuum level is below the conduction band minimum. In other words, the ionization potential is smaller than the band gap. A

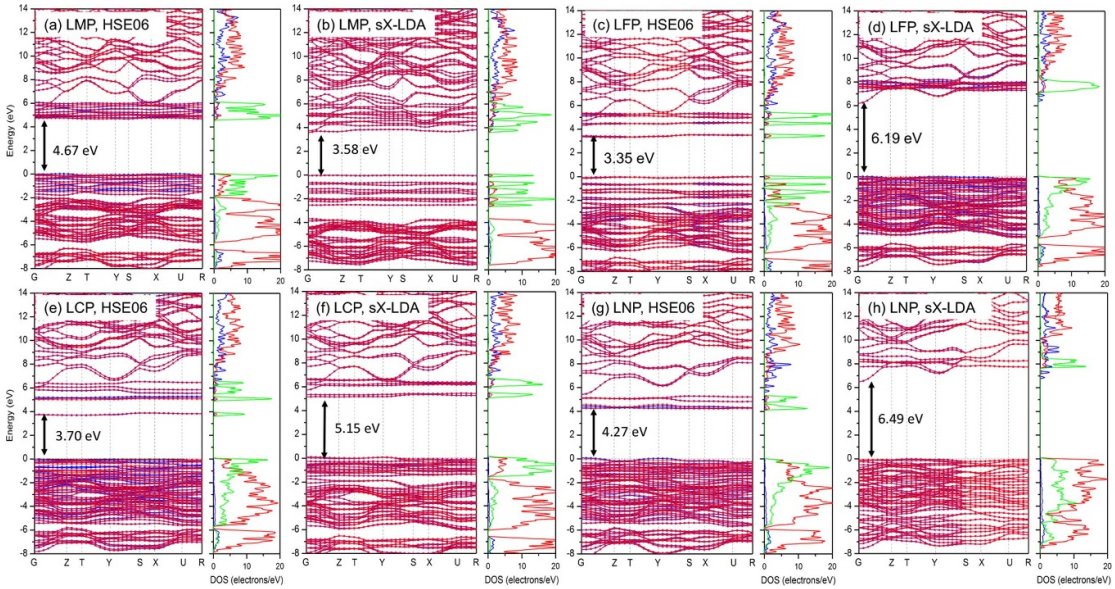


**Figure 4.** Calculated electronic band structure (left panels) and DOS (right panels) for $LiMPO_4$ with HSE06 and sX-LDA. (a) and (b) M = Mn; (c) and (d) M = Fe; (e) and (f) M = Co; (g) and (h) M = Ni. The blue, red and green lines on the right panels represent the s, p and d density of states. Reprinted (adapted) with permission from [23]. Copyright (2020) American Chemical Society.

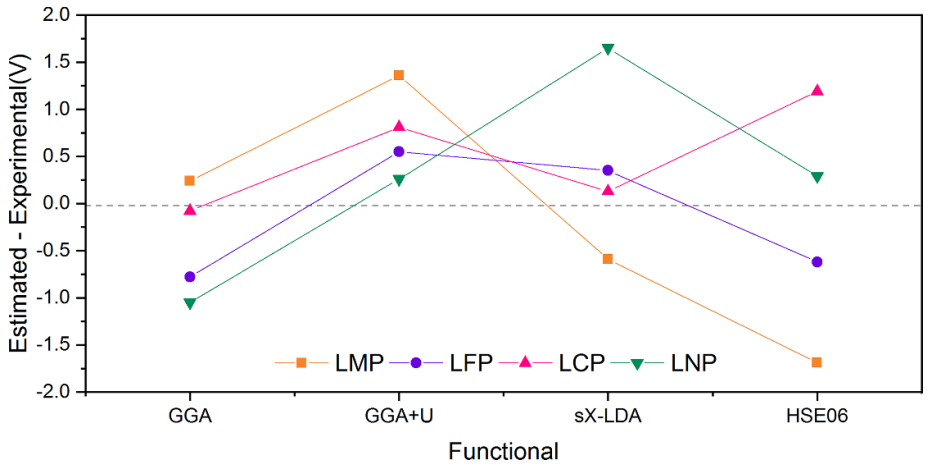


**Figure 5.** Differential between calculated and experimental Li intercalation voltage for $LiMPO_4$ with various functionals. Reprinted (adapted) with permission from [23]. Copyright (2020) American Chemical Society.

measured ionization potential of 5.98 eV further confirms that the calculated and experimentally determined band-gap value of 6.2–6.3 eV (>5.98 eV) is likely to be a more correct determination of LFP properties [19].

Since Li extraction is accompanied by the removal of electrons from the valence band maximum (VBM), a study of the VBM is also important. The VBM of all olivine phosphates is dominated by TM-3d states hybridizing with O-2p states with HSE06 functional calculations, while O-2p states dominate the VBM of LNP calculated with the sX-LDA functional. This apparent dichotomy may also arise from the abovementioned LNP .cif files, with large residual non-equilibrium forces, affecting the electron density distributions.

Besides the electronic band structure alignment, Li intercalation voltages have been used for further comparison and validation of these approaches to delineate electronic behaviour of olivine phosphates. The estimated Li intercalation voltages of $LiMPO_4$ are compared with experimental values in figure 5. Overall, calculated results obtained with the sX-LDA functional show the best accuracy for the estimated Li intercalation voltages of LMP, LFP and LCP, except for LNP.

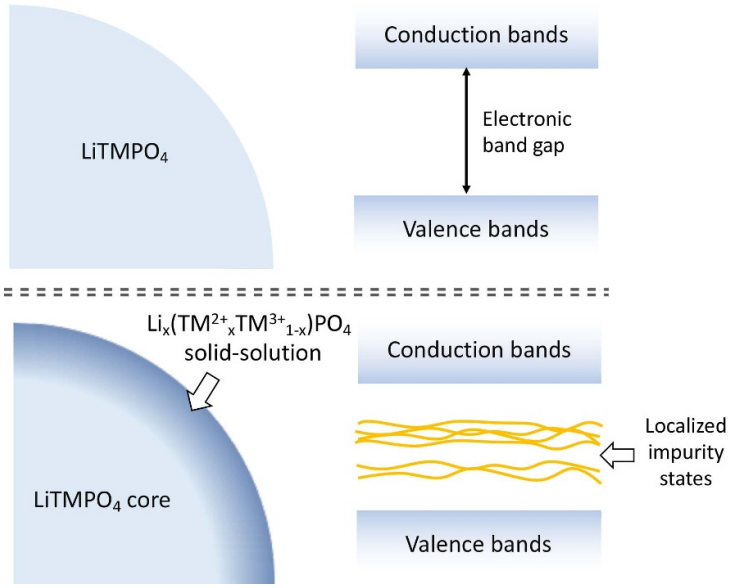


**Figure 6.** Schematic of the core–shell structure and its effect on the electronic band structure. Reprinted (adapted) with permission from [21]. Copyright (2020) American Chemical Society.

## 5. Surface chemistry, optical absorption and electronic band structure

As mentioned above, surface chemistry has a profound influence on the optical absorption properties of $LiMPO_4$. Hence, this chemistry also affects the electronic band structure; an understanding of which is critical to detailed knowledge of electronic transport mechanisms and of band alignment between cathodes and electrolytes. A schematic showing this influence is illustrated in figure 6. As shown in the estimated electronic band structure, $LiMPO_4$ materials with perfect crystal structure are expected to have clear band gaps, that give sharp, well-defined absorption edges in optical absorption spectra. Intervalence charge transfer has been confirmed experimentally and explained theoretically in the literature [38] for $Li_{0.6}\left(Fe^{2+}_{0.6}Fe^{3+}_{0.4}\right)PO_4$ solid-solution, as the $Fe^{3+}$-3d states fall in the gap between $Fe^{2+}$-3d states. A similar story can also be expected for the mixed oxidation states of TM on the surface, resulting in localized TM-3d impurity states inside the band gap of bulk $LiMPO_4$. This condition would lead to an intermediate absorption peak value and large Urbach tails in the optical absorption spectra of these samples.

In earlier investigations [26] the ionic and electronic conduction mechanisms of $LiMPO_4$ are considered to be via diffusion of Li vacancies and hopping of small polarons. The small polaron in olivine phosphates can be considered as a d-hole on $TM^{3+}$ that can hop onto a neighbouring $TM^{2+}$ (and turn it into $TM^{3+}$ leaving behind $TM^{2+}$). Therefore, surface chemistry, such as the concentration of Li vacancies and the ratio of $TM^{2+}/TM^{3+}$, must have a significant impact on the surface electronic and ionic conduction of $LiMPO_4$, and ultimately on bulk electrochemical performance.

## 6. Preferential surface doping of LFP

After re-evaluating the properties and characteristics of pristine materials, a series of cation doped LFP, which was previously reported as beneficial to the rate capability, has also been investigated [22]. The surface chemistry has been characterized with XPS and sXAS as shown in figure 7. The concentration of $Fe^{3+}$ on the sample surfaces increases with the addition of cation dopants, while the cores remain similar to the original stoichiometric samples. This relationship suggests that the effect of cation doping is more significant on the surface of the LFP than within the bulk. The $LiMPO_4$ olivine structure has been reported as having no tolerance for aliovalent doping on either Li or TM sites due to high solution energy [49], although there are numerous reports on experimental doping success, resulting in improved rate capability [14, 50–56]. We suggest it is likely that the cation dopants are pushed to the particle surfaces during phase formation, which intensifies the surface distortion of LFP particles. Similar surface accumulation of dopants has been reported in Fe substituted $LiCoPO_4$ samples [57]. Uniform distribution of the dopants can only be achieved when the sample is fast annealed (heating up to 650 °C in 3 min and cooling down to room temperature in 20 min) [57]. Furthermore, significant drops in charge transfer resistance and polarization have been found for the

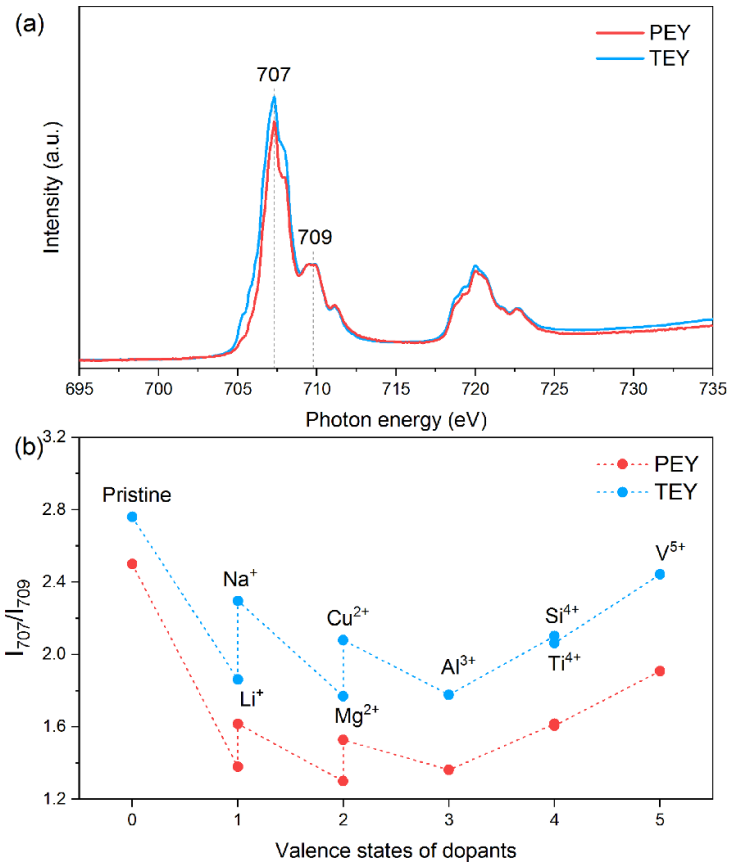


**Figure 7.** (a) Fe-L edge of the pristine LFP sample acquired with PEY and TEY modes. (b) Intensity ratio of the 707 and 709 peaks for the pristine and doped LFP samples. Dopants appear to enhance not only the surface oxidation but also the oxidation concentration gradient, resulting in slight variations of the intensity ratios of the 707 and 709 peaks. Reprinted (adapted) with permission from [22]. Copyright (2020) American Chemical Society.

doped LFP samples in our study. These effects suggest a more favourable surface for charge transfer has been obtained [20] due to surface dopant segregation.

## 7. Junction effects on particle surfaces

As mentioned above, DFT calculations of the electronic band structures for LFP and FePO4 using the sX-LDA functional closely match experimentally measured values for their respective band gaps. This convergence of calculation and experiment also applies to results on work functions and ionization potentials for these compounds [58]. Based on these results, the schematic in figure 8 summarizes the approximate relative positions of energy levels for the core and the surface of LFP particles: (a) prior to, and (b) after, placing them in contact. The $FePO_4$ band structure has empty levels just above the Fermi level, due to an odd $d^5$ configuration of the Fe-ions [19]. Some electrons from LFP will be transferred to the $FePO_4$, resulting in an effective *p*-doping and *n*-doping of LFP and FP, respectively. Some possible *p*–*n* junction effects in LFP battery materials have been discussed in an earlier publication [59].

Carbon coating is also part of the surface nanostructure of LFP materials [24]. The work function of carbon is reported to be very dependent on the specific type of carbon. For example, the work function can vary within a wide range covering <1 eV and about 5–6 eV [60]. In particular, it has been shown that doping of carbon itself with other ions is able to reduce the value of the work function [61]. Bulk analyses of LFP materials typically undertaken using inductively coupled plasma optical emission spectroscopy analyses, often show a slight excess of Li [20, 23]. Since this excess Li is not in the core LFP structure, let alone on the de-lithiated surface (as shown above), it is likely that small amounts are doped into the amorphous carbon coating. Preliminary DFT calculations on work functions for different carbons indicate values around 5 eV for either graphitic or amorphous carbon without doping. Li-doping appears to reduce the calculated work function value to ~3.5 eV. Such work functions, if equal or under 3.5 eV, will position the Fermi level of the amorphous conducting carbon ideally for good ohmic contact [62]. Good ohmic contact is no doubt an essential condition for improved electrochemical performance. More detailed theoretical and experimental

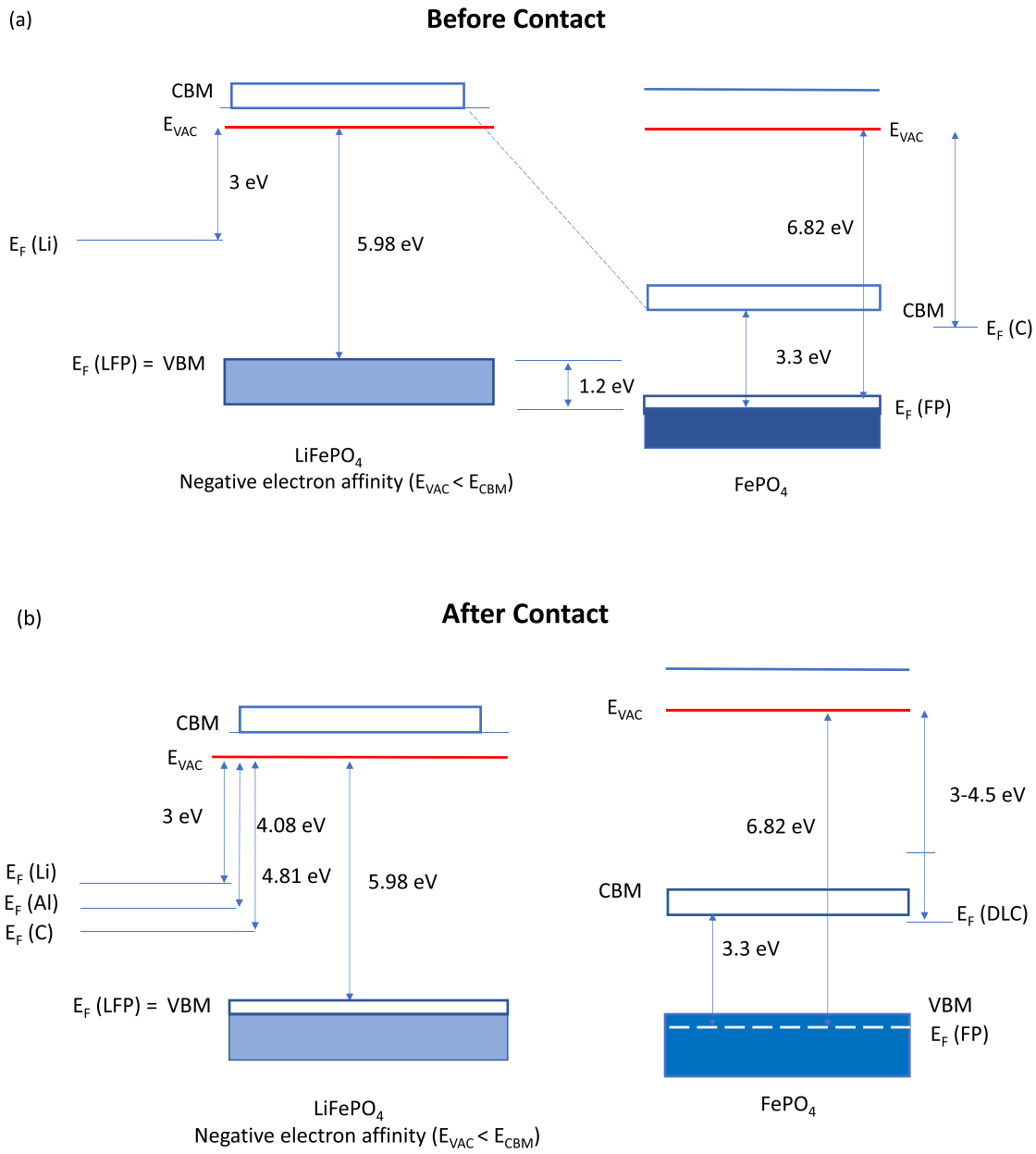


**Figure 8.** Schematic relative positions of the energy levels for the surface and the core of LFP particles: (a) before contact (b) after contact. In this figure, $E_F$ corresponds to the Fermi level position attributed by DFT calculations of the electronic band structures. This position is different from the Fermi level used for work function determination of semiconductors and insulators (gapped materials) using UPS.

investigations on work functions of amorphous carbon are currently underway and will be published separately.

## 8. Conclusions and perspectives

The effects of surface chemistry on the electronic and ionic conductivities of $LiMPO_4$ compounds are real, detectable and calculable. Thus, surface nanostructures and their optimization should be considered at every level of material design, characterization, modification and testing. A more recent study on the solid-solution $Li_{0.5}FePO_4$ has also confirmed the importance of particle surfaces in electrochemical processes. Li ions have been found to migrate along the solid/liquid interface, without leaving the particle surfaces [63]. This mechanism appears to take place during both lithiation and de-lithiation and to control the phase transformation rate in $Li_xFePO_4$.

Since surface differentiation from the core has been observed in this research, junction effects between the surface and core of particles, and even the conductive carbon surface coating, may be expected. Thorough and quantitative understanding of the contributions from all the components and interfaces on

the electronic structure and transport mechanisms, including all the electronic band structure, work function and ionization potential alignments, is required.

Our preliminary studies on lithium nickel manganese cobalt oxides (NMC) show that similar differential nanostructures from surface to bulk are also present [18]. Therefore, investigations on the surface properties and the effect on the electrochemical performance of these compounds should be extended to NMC and, quite probably, to other electrode materials. Overall, differentiated surfaces from the cores appear to be a significant characteristic of cathode materials that influences measured properties. Thus, inclusive design of cathode surfaces can provide new ideas for optimization of performance and cyclability of battery materials.

## Acknowledgments

Y Zhang would like to acknowledge CSIRO for the studentship, with involvement of CRRC and the Rail Manufacturing Cooperative Research Centre (funded jointly by participating rail organisations and the Australian Federal Government's Cooperative Research Centres Program). The experimental data were obtained at the Central Analytical Research Facility operated by the Institute for Future Environments, Queensland University of Technology (QUT), Brisbane, Australia. The authors acknowledge Dr Michael Jones, QUT, for the assistance with the proposal for Australian Synchrotron beamline application and the Australian Synchrotron for the awarded beamtime. Computational resources and services used in this work were provided by the HPC and Research Support Group, eResearch Office, QUT. Partial support was also provided from the Australian Renewable Energy Agency (ARENA) Research and Development Program—Renewable Hydrogen for Export (Contract No. 2018/RND012).

## ORCID iDs

Y Zhang https://orcid.org/0000-0003-4717-9899
J A Alarco https://orcid.org/0000-0001-6345-071X
M Khosravi https://orcid.org/0000-0002-7272-3641
I D R Mackinnon https://orcid.org/0000-0002-0732-8987

## References

[1] Padhi A K, Nanjundaswamy K and Goodenough J B 1997 Phospho-olivines as positive-electrode materials for rechargeable lithium batteries *J. Electrochem. Soc.* **144** 1188–94
[2] Oh S-M, Oh S-W, Yoon C-S, Scrosati B, Amine K and Sun Y-K 2010 High-performance carbon-$LiMnPO_4$ nanocomposite cathode for lithium batteries *Adv. Funct. Mater.* **20** 3260–5
[3] Wolfenstine J, Lee U, Poese B and Allen J L 2005 Effect of oxygen partial pressure on the discharge capacity of $LiCoPO_4$ *J. Power Sources* **144** 226–30
[4] Prabu M, Selvasekarapandian S, Kulkarni A R, Karthikeyan S, Hirankumar G and Sanjeeviraja C 2011 Structural, dielectric, and conductivity studies of yttrium-doped $LiNiPO_4$ cathode materials *Ionics* **17** 201–7
[5] Wang Y, He P and Zhou H 2011 Olivine $LiFePO_4$: development and future *Energy Environ. Sci.* **4** 805–17
[6] Ravet N, Chouinard Y, Magnan J, Besner S, Gauthier M and Armand M 2001 Electroactivity of natural and synthetic triphylite *J. Power Sources* **97** 503–7
[7] Doeff M M, Wilcox J D, Kostecki R and Lau G 2006 Optimization of carbon coatings on $LiFePO_4$ *J. Power Sources* **163** 180–4
[8] Li J, Zhang L, Zhang L, Hao W, Wang H, Qu Q and Zheng H 2014 *In-situ* growth of graphene decorations for high-performance $LiFePO_4$ cathode through solid-state reaction *J. Power Sources* **249** 311–9
[9] Malik R, Burch D, Bazant M and Ceder G 2010 Particle size dependence of the ionic diffusivity *Nano Lett.* **10** 4123–7
[10] Kim D-H and Kim J 2006 Synthesis of $LiFePO_4$ nanoparticles in polyol medium and their electrochemical properties *Electrochem. Solid-State Lett.* **9** A439–42
[11] Kitao H, Fujihara T, Takeda K, Nakanishi N and Nohma T 2005 High-temperature storage performance of Li-ion batteries using a mixture of Li-Mn spinel and Li-Ni-Co-Mn oxide as a positive electrode material *Electrochem. Solid-State Lett.* **8** A87–90
[12] Kosova N V, Devyatkina E T and Kaichev V V 2009 $LiMn_2O_4$ and $LiCoO_2$ composite cathode materials obtained by mechanical activation *Russ. J. Electrochem.* **45** 277–85
[13] Wang Y, Wang Y, Hosono E, Wang K and Zhou H 2008 The design of a $LiFePO_4$/Carbon nanocomposite with a core–shell structure and its synthesis by an in situ polymerization restriction method *Angew. Chem., Int. Ed.* **47** 7461–5
[14] Chung S Y, Bloking J T and Chiang Y M 2002 Electronically conductive phospho-olivines as lithium storage electrodes *Nat. Mater.* **1** 123–8
[15] Xu Z, Gao L, Liu Y and Li L 2016 Review—recent developments in the doped $LiFePO_4$ cathode materials for power lithium ion batteries *J. Electrochem. Soc.* **163** A2600–10
[16] Li H, Wang Z, Chen L and Huang X 2009 Research on advanced materials for Li-ion batteries *Adv. Mater.* **21** 4593–607
[17] Benedek P, Yazdani N, Chen H, Wenzler N, Juranyi F, Månsson M, Islam M S and Wood V C 2019 Surface phonons of lithium ion battery active materials *Sustain. Energy Fuels* **3** 508–13
[18] Zhang Y 2020 Study on electronic structure and rate performance of olivine phosphate cathode materials PhD Thesis Queensland University of Technology
[19] Zhang Y, Alarco J A, Best A S, Snook G A, Talbot P C and Nerkar J Y 2019 Re-evaluation of experimental measurements for the validation of electronic band structure calculations for $LiFePO_4$ and $FePO_4$ *RSC Adv.* **9** 1134–46

[20] Zhang Y, Alarco J A, Nerkar J Y, Best A S, Snook G A and Talbot P C 2019 Improving the rate capability of $LiFePO_4$ electrode by controlling particle size distribution *J. Electrochem. Soc.* **166** A4128–35

[21] Zhang Y, Alarco J A, Nerkar J Y, Best A S, Snook G A, Talbot P C and Cowie B C C 2020 Spectroscopic evidence of surface Li-depletion of lithium transition metal phosphates *ACS Appl. Energy Mater.* **3** 2856–66

[22] Zhang Y, Alarco J A, Nerkar J Y, Best A S, Snook G A, Talbot P C and Cowie B C C 2020 Observation of preferential cation doping on the surface of $LiFePO_4$ particles and its effect on properties *ACS Appl. Energy Mater.* **3** 9158–67

[23] Zhang Y, Alarco J A, Nerkar J Y, Best A S, Snook G A, Talbot P C and Cowie B C C 2020 Effects of nanoscale surface lithium depletion on the optical properties and electronic band structures of lithium transition-metal phosphates *J. Phys. Chem.* C **124** 19969–79

[24] Zhang Y, Alarco J A, Nerkar J Y, Best A S, Snook G A and Talbot P C 2020 Nanoscale characteristics of practical $LiFePO_4$ materials—effects on electrical, magnetic and electrochemical properties *Mater. Charact.* **162** 110171

[25] Deng S, Wang H, Liu H, Liu J and Yan H 2014 Research progress in improving the rate performance of $LiFePO_4$ cathode materials *Nano-Micro Lett.* **6** 209–26

[26] Hoang K and Johannes M 2011 Tailoring native defects in $LiFePO_4$: insights from first-principles calculations *Chem. Mater.* **23** 3003–13

[27] Yamada A and Chung S-C 2001 Crystal chemistry of the olivine-type $Li(Mn_yFe_{1-y})PO_4$ and $(Mn_yFe_{1-y})PO_4$ as possible 4 V cathode materials for lithium batteries *J. Electrochem. Soc.* **148** A960–7

[28] Tang X-C, Li L-X, Lai Q-L, Song X-W and Jiang L-H 2009 Investigation on diffusion behavior of Li+ in $LiFePO_4$ by capacity intermittent titration technique (CITT) *Electrochim. Acta* **54** 2329–34

[29] Morgan D, van Der Ven A and Ceder G 2004 Li conductivity in $Li_xMPO_4$ (M = Mn, Fe, Co, Ni) olivine materials *Electrochem. Solid-State Lett.* **7** A30–2

[30] Fisher C A, Hart Prieto V M and Islam M S 2008 Lithium battery materials $LiMPO_4$ (M = Mn, Fe, Co, and Ni): insights into defect association, transport mechanisms, and doping behavior *Chem. Mater.* **20** 5907–15

[31] Yamada A, Takei Y, Koizumi H, Sonoyama N, Kanno R, Itoh K, Yonemura M and Kamiyama T 2006 Electrochemical, magnetic, and structural investigation of the $Li_x(Mn_yFe_{1-y})PO_4$ olivine phases *Chem. Mater.* **18** 804–13

[32] Safari M and Delacourt C 2011 Aging of a commercial graphite/$LiFePO_4$ cell *J. Electrochem. Soc.* **158** A1123–35

[33] Li G, Azuma H and Tohda M 2002 $LiMnPO_4$ as the cathode for lithium batteries *Electrochem. Solid-State Lett.* **5** A135–7

[34] Amine K, Yasuda H and Yamachi M 2000 Olivine $LiCoPO_4$ as 4.8 V electrode material for lithium batteries *Electrochem. Solid-State Lett.* **3** 178–9

[35] Rousse G, Rodriguez-Carvajal J, Patoux S and Masquelier C 2003 Magnetic structures of the triphylite $LiFePO_4$ and of its delithiated form $FePO_4$ *Chemi. Mater.* **15** 4082–90

[36] Zhou F, Kang K, Maxisch T, Ceder G and Morgan D 2004 The electronic structure and band gap of $LiFePO_4$ and $LiMnPO_4$ *Solid State Commun.* **132** 181–6

[37] Zaghib K, Mauger A, Goodenough J B, Gendron F and Julien C 2007 Electronic, optical, and magnetic properties of $LiFePO_4$: small magnetic polaron effects *Chem. Mater.* **19** 3740–7

[38] Furutsuki S, Chung S-C, Nishimura S-I, Kudo Y, Yamashita K and Yamada A 2012 Electrochromism of $Li_xFePO_4$ induced by intervalence charge transfer transition *J. Phys. Chem.* C **116** 15259–64

[39] Hunt A, Ching W Y, Chiang Y M and Moewes A 2006 Electronic structures of $LiFePO_4$ and $FePO_4$ studied using resonant inelastic x-ray scattering *Phys. Rev.* B **73** 205120

[40] Augustsson A, Zhuang G V, Butorin S M, Osorio-Guillen J M, Dong C L, Ahuja R, Chang C L, Ross P N, Nordgren J and Guo J H 2005 Electronic structure of phospho-olivines $Li_xFePO_4$ ($x = 0$, 1) from soft-x-ray-absorption and -emission spectroscopies *J. Chem. Phys.* **123** 184717

[41] Piper L F J *et al* 2013 Elucidating the nature of pseudo Jahn–Teller distortions in $Li_xMnPO_4$: combining density functional theory with soft and hard X-ray spectroscopy *J. Phys. Chem.* C **117** 10383–96

[42] McBreen J 2009 The application of synchrotron techniques to the study of lithium-ion batteries *J. Solid State Electrochem.* **13** 1051–61

[43] Nakanishi K and Ohta T 2012 Improvement of the detection system in the soft X-ray absorption spectroscopy *Surf. Interface Anal.* **44** 784–8

[44] Clark S J and Robertson J 2010 Screened exchange density functional applied to solids *Phys. Rev.* B **82** 085208

[45] Gillen R and Robertson J 2013 Accurate screened exchange band structures for the transition metal monoxides MnO, FeO, CoO and NiO *J. Condens. Matter Phys.* **25** 165502

[46] Warda S A and Lee S-L 1997 Refinement of the crystal structure of lithium nickel phosphate, $LiNiPO_4$ *Z. Kristallogr.* **212** 319

[47] Ramana C V, Ait-Salah A, Utsunomiya S, Becker U, Mauger A, Gendron F and Julien C M 2006 Structural characteristics of lithium nickel phosphate studied using analytical electron microscopy and Raman spectroscopy *Chem. Mater.* **18** 3788–94

[48] Abrahams I and Eassons K S 1993 Structure of lithium nickel phosphate *Acta Cryst.* **C41** 1–4

[49] Islam M S, Driscoll D J, Fisher C A and Slater P R 2005 Atomic-scale investigation of defects, dopants, and lithium transport in the $LiFePO_4$ olivine-type battery material *Chemi. Mater.* **17** 5085–92

[50] Delacourt C, Wurm C, Laffont L, Leriche J B and Masquelier C 2006 Electrochemical and electrical properties of Nb- and/or C-containing $LiFePO_4$ composites *Solid State Ion.* **177** 333–41

[51] Yang L, Jiao L, Miao Y and Yuan H 2009 Synthesis and characterization of $LiFe_{0.99}Mn_{0.01}(PO_4)_{2.99/3}F_{0.01}$/C as a cathode material for lithium-ion battery *J. Solid State Electrochem.* **14** 1001–5

[52] Zhang Q, Wang S, Zhou Z, Ma G, Jiang W, Guo X and Zhao S 2011 Structural and electrochemical properties of Nd-doped $LiFePO_4$/C prepared without using inert gas *Solid State Ion.* **191** 40–4

[53] Ban C, Yin W-J, Tang H, Wei S-H, Yan Y and Dillon A C 2012 A novel codoping approach for enhancing the performance of $LiFePO_4$ cathodes *Adv. Energy Mater.* **2** 1028–32

[54] Wang Z-H, Yuan L-X, Ma J, Qie L, Zhang L-L and Huang Y-H 2012 Electrochemical performance in Na-incorporated nonstoichiometric $LiFePO_4$/C composites with controllable impurity phases *Electrochim. Acta* **62** 416–23

[55] Hu C L, Yi H H, Wang F X, Xiao S Y, Wu Y P, Wang D and He D L 2014 Boron doping at P-site to improve electrochemical performance of $LiMnPO_4$ as cathode for lithium ion battery *J. Power Sources* **255** 355–9

[56] Kulka A, Braun A, Huang T-W, Wolska A, Klepka M T, Szewczyk A, Baster D, Zając W, Świerczek K and Molenda J 2015 Evidence for Al doping in lithium sublattice of $LiFePO_4$ *Solid State Ion.* **270** 33–8

[57] Okita N *et al* 2018 Stabilizing the structure of $LiCoPO_4$ nanocrystals via addition of $Fe^{3+}$: formation of $Fe^{3+}$ surface layer, creation of diffusion-enhancing vacancies, and enabling high-voltage battery operation *Chem. Mater.* **30** 6675–83

[58] Alarco J A E A 2020 *preparation*
[59] Kalantharian M M, Asgari S and Mustarelli P 2014 A theoretical approach to evaluate the rate capability of Li-ion battery cathode materials *J. Mater. Chem.* A **2** 107–15
[60] Neuville S 2014 New application perspective for tetrahedral amorphous carbon coatings *QScience Connect* **8** 1–27
[61] Akada K, Obata S and Saiki K 2019 Work function lowering of graphite by sequential surface modifications: nitrogen and hydrogen plasma treatment *ACS Omega* **4** 16531–5
[62] Kao K C 2004 *Dielectric Phenomena in Solids* (San Diego, CA: Academic)
[63] Li Y *et al* 2018 Fluid-enhanced surface diffusion controls intraparticle phase transformations *Nat. Mater.* **17** 915–22